Highly selective, reusable electrochemical impedimetric DNA sensors based on carbon nanotube/polymer composite electrode without surface modification

Huaide Jiang, Eun-Cheol Lee

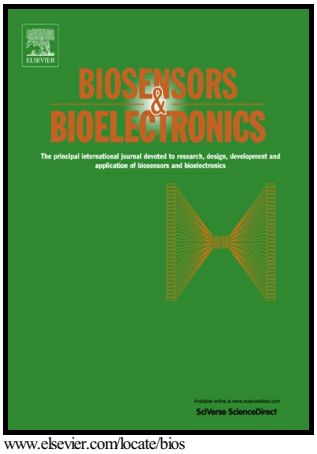

www.elsevier.com/locate/bios

PII: S0956-5663(18)30531-1
DOI: https://doi.org/10.1016/j.bios.2018.07.037
Reference: BIOS10626

To appear in: *Biosensors and Bioelectronic*

Received date: 14 May 2018
Revised date: 2 July 2018
Accepted date: 16 July 2018

Cite this article as: Huaide Jiang and Eun-Cheol Lee, Highly selective, reusable electrochemical impedimetric DNA sensors based on carbon nanotube/polymer composite electrode without surface modification, *Biosensors and Bioelectronic,* https://doi.org/10.1016/j.bios.2018.07.037

Highly selective, reusable electrochemical impedimetric DNA sensors based on carbon nanotube/polymer composite electrode without surface modification

Huaide Jiang,[a,c] Eun-Cheol Lee[a,b,c,*]

[a]*Department of Nano Science and Technology, Gachon University, Gyeonggi 13120, Republic of Korea*

[b]*Department of Nano-Physics, Gachon University, Gyeonggi 13120, Republic of Korea*

[c]*Gachon Bio-Nano Research, Gachon University, Gyeonggi 13120, Republic of Korea*

*Corresponding author at: Gachon University, Department of Nano-Physics, 1342 SeongnamDaero, Sujeong-Gu, Seongnam, Gyeonggi 13120, Republic of Korea. Tel.: +82 31 750 8752; Fax: +82 31 750 8769. *E-mail address*: eclee@gachon.ac.kr (E.-C. Lee).

Abstract

We fabricated a composite of multi-walled carbon nanotube and polydimethylsiloxane and utilized it as an electrode for DNA sensing using electrochemical impedance spectroscopy. Without any surface modification or probe immobilization, often necessary for other electrodes, this electrode also acts as a recognition layer for DNA via π-π interactions between the multi-walled carbon nanotube and DNA. This electrode is easily reusable via a simple cleansing process, because there are no

covalently bonded adsorbates on the electrode. Compared to previous DNA detection based on differential pulse voltammetry using a similar electrode, the measurement time was reduced from 1 h to less than 30 min, and the limit of detection (25 pM) was reduced by a factor of more than five. In addition, our system can detect the single-base mismatch between the target and probe. Our results indicate that electrochemical impedance spectroscopy is promising for utilizing the multi-walled carbon nanotube and polydimethylsiloxane electrode as a DNA sensor.

Keywords: biosensor, carbon nanotube, polydimethylsiloxane, impedance

1. Introduction

Recently, DNA sensors have attracted considerable attention because of their applications to genetic screening and detection (Garrido-Cardenas, et al., 2017; Heller, M.J, 2002; Mcglennen, R. C, 2001). Despite intensive studies thus far, it is still desirable to develop more stable, sensitive, and rapidly detecting sensors. Recently, because fluorescence-based sensors require an inefficient dye labelling process, many efforts have been made to develop label-free DNA sensors. As an alternative to fluorescence-based sensors, electrochemical DNA sensors have been widely studied (Galan et al., 2015; Peng et al., 2015; Cui et al., 2017). They have shown high sensitivity, rapid response, and ease of miniaturization (Drummond et al., 2003; Chen et al., 2016). Particularly, electrochemical impedance spectroscopy (EIS) is promising for applications in DNA detection because it can detect biologic interaction near the electrode surface, which is easily applicable to label-free DNA detection (Brett et al.,

1999; Fu et al., 2005; Gong., et al., 2017; Keighley et al., 2008). Typically, gold has been used as a working electrode in EIS-based DNA sensors (Hassen et al., 2008; Li et al., 2007). However, gold is very expensive, and thus is disadvantageous for commercialization of sensors. In addition, these sensors also usually require probe immobilization on the gold surface, which is sometimes time-consuming and laborious. As a less expensive alternative to gold electrodes, glassy carbon electrodes (GCEs) have also been widely studied. To use GCEs for EIS-based DNA detection, surface modification using other materials such as gold nanoparticles (Gupta et al., 2013; Yang et al., 2007) is required. In addition, probe immobilization of the electrode is still needed (Gupta et al., 2013; Hassen et al., 2008; Li et al., 2007; Yang et al., 2007).

On the other hand, following the first discovery of carbon nanotubes (CNTs) by Iijima in 1991 (Iijima, 1991), their unique electrical, chemical, mechanical, and thermal properties have been intensively studied during recent years (Huang et al., 2014; Khan et al., 2014; Ramanathan et al., 2016). Particularly, there has been considerable interest in using CNTs as a surface modifier for GCEs in EIS-based DNA detection. Xu and coworkers reported EIS-based DNA detection using polypyrrole / multi-walled carbon nanotubes (MWCNTs) for modifying GCEs (Xu et al., 2006). Weber and coworkers studied an electrochemical-impedance-based DNA sensor by modifying a GCE with a single-walled CNT (Weber et al., 2011). Similar to the probe immobilization process, such a surface modification of a GCE using CNTs is usually complicated, sophisticated, and laborious. Regarding commercialization,

surface modification and probe immobilization processes can possibly increase production costs, limit mass production, and cause large variations in performance because of the very sensitive nature of the processes. To the best of our knowledge, CNTs have not been used yet as the main material of electrodes for EIS-based DNA detection.

In this work, we fabricated a composite electrode of MWCNT and polydimethylsiloxane (PDMS), which was utilized for highly selective detection of DNA using EIS. This sensor is based on the physisorption of DNA on the MWCNT surfaces via π-π interactions and, thus, does not require any surface modification or probe immobilization (Fig. 1a). Because MWCNTs are chemically very inert and the physisorbed DNA can be easily removed from their surfaces, our MWCNT-based sensor is easily reusable via a simple cleansing process. Compared to DNA sensing based on previous differential voltammetry using a similar electrode (Li and Lee, 2015), the measurement time was reduced from 1 h to less than 30 min and the limit of detection decreased from 130 pM to 25 pM. These results indicate that EIS is promising for utilizing the MWCNT/PDMS electrode in DNA sensing.

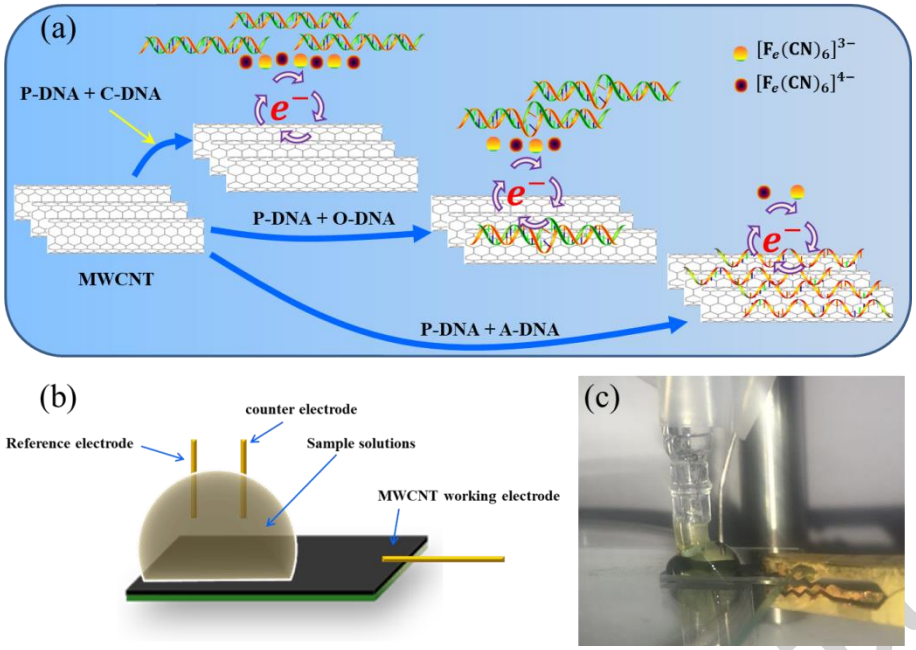

Fig. 1 (a) Schematic diagram of our impedance-based DNA sensor. (b) Schematic and (b) photograph of the experimental setup.

2. Materials and methods

2.1 Reagents and materials

MWCNTs (diameter: 10–15 nm; length: 30–40 μm) were purchased from HANOS (South Korea). DNA sequences including probe DNA (P-DNA), complementary target DNA (C-DNA), one-base-mismatched target DNA (O-DNA) and all-base-mismatched target DNA (A-DNA) were ordered from Bioneer (South Korea) (see Table S1). PDMS was purchased from Sigma-Aldrich (USA). Potassium hexacyanoferrate ($K_3Fe(CN)_6$) was purchased from Junsei Chemical Co., Ltd (Tokyo, Japan). Potassium hexacyanoferrate trihydrate ($K_4Fe(CN)_6$) was purchased from Sigma-Aldrich (USA). 2-propanol (IPA) solution was purchased from J.T. Baker (USA). 1 × phosphate buffered saline (1 ×PBS) solution (PH=7.4) was purchased

from Tech and Innovation Corporation (South Korea). The resistivity of the de-ionized water used throughout this study was 18.2 MΩ·cm. All other chemicals were analytical-reagent grade.

2.2 Instruments

EIS and cyclic voltammetry (CV) were performed using a VersaSTAT 4 (Princeton Applied Research, Inc. USA). A probe sonicator (HD 2070, Bandelin, Germany) was used for dispersing the MWCNTs in the IPA solution. Ultraviolet (UV) absorption spectroscopy was measured using a UV-visible spectrophotometer (Cary 50, Varian, Australia). Surface morphology and cross-section images of the MWCNT/PDMS electrodes were obtained using scanning electron microscopy (SEM; S4800, Hitachi, Japan). The Ag/AgCl reference electrode, in which the potential with respect to the standard hydrogen electrode is 0.197 V, and platinum wire (counter) electrode were purchased from Princeton Applied Research (USA).

2.3 Preparation of the MWCNT/PDMS electrode

The fabrication process of the MWCNT/PDMS composite electrode is summarized in Fig. S1, and is similar to that of our previous study (Li and Lee, 2015). First, 16 mg of MWCNT powder was dispersed in 20 ml of anhydrous IPA solution via tip sonication for 30 min. The MWCNT layer was formed via three cycles of casting and drying of the MWCNT solution. During the first cycle, 10 mL of the solution was placed onto a petri dish at a diameter of 85 mm and dried at 95°C for 40 min. During the second and the third cycles, 5 mL of the solution was used and the drying time

was 30 min. 10 g of PDMS was prepared by mixing an elastomer and curing agent in a weight ratio of 10:1 and placed in a vacuum pump to remove air bubbles. Then, PDMS was poured onto the dry MWCNT layer. A film thickness of approximately 260 μm was obtained by covering the glass substrate on the film with MWCNTs and PDMS at 95°C for 10 h; the thickness was measured using SEM, which will be discussed later in this paper. In contrast to our previous study (Li and Lee, 2015), extra pressure was not exerted on the glass to make the film sufficiently thick to prevent self-curling of the film. Finally, the MWCNT/PDMS electrode was cut to 15 mm × 5 mm. The as-made MWCNT/PDMS electrode was cleaned by sonicating it in absolute ethanol and DI water for 5 min, in turn, and then was maintained in an oven at 60 °C before use. It is noteworthy that good reagents for dispersing MWCNTs have proved to be N-Methyl-2-pyrrolidone (NMP) or dimethylformamide (DMF) (Bergin et al., 2010). However, the high boiling points of NMP (202 °C) and DMF (153 °C) make it difficult to separate MWCNTs from NMP or DMF via heat, and both the NMP and DMF reagents are harmful to the human body. Considering this, we chose an anhydrous IPA solution to disperse the MWCNTs. Because our fabrication of the MWCNT/PDMS electrode was achieved by casting PDMS onto the MWCNT layer, the density of the MWCNT on the MWCNT-rich side in our film may be much higher than that of films obtained by direct mixing of MWCNTs and PDMS (Noimark et al., 2016; Pumera et al., 2006).

To check if the amount of MWCNTs was optimized, electrodes with various concentrations of MWCNT were fabricated. Then, immersing the MWCNT, Ag/AgCl,

and platinum electrode into 1 mL of PBS solution, containing 4 mM potassium ferricyanide/potassium ferrocyanide redox couple ($[Fe(CN)_6]^{3-}/[Fe(CN)_6]^{4-}$ (see Fig. S2), CV measurements were performed at a scan rate 0.1 V s^{-1} between the potentials 0.8 and -0.5 V as shown in Fig. 2a. Figure 2b shows the peak voltage separation (ΔE_p) and anodic peak current (I_{pa}) versus the amount of MWCNTs**.** Similar to previous studies (Pumera et al., 2006), a decrease in ΔE_p and increase in I_{pa} accompanied an increase in the amount of MWCNTs, indicating that more MWCNTs are better for a larger current response. However, when the MWCNT was equal to or more than 18 mg, it was easy to peel from the PDMS layer, thereby affecting the stability of the electrode. Thus, 16 mg was chosen to be the mass of the MWCNT during our standard fabrication process, which showed a ΔE_p as low as 0.15 V and a well-defined, developed I_{pa}. Because EIS also relies on the charge transfer from $[Fe(CN)_6]^{3-}/[Fe(CN)_6]^{4-}$ to the electrode, the optimized electrode with CV might also be good for EIS.

No obvious capacitive currents were observed in the CV curves in Fig. 2a. This might be attributed to the fact that PDMS covered a large fraction of the electrode surface, as shown in Fig. 3b, suppressing formation of capacitive double layers. To further validate this idea, we prepared pure MWCNT electrode without PDMS, by cutting the MWCNT-deposited petri dish, which was prepared through three cycles of casting and drying of the MWCNT solution as discussed above, into the electrode size. CV of this electrode showed substantial amount of capacitive current, as shown in Fig. S3, indicating that PDMS plays an important role in suppressing the capacitance. The

capacitance character of bare MWCNT is detrimental to quantitative DNA detection. Moreover, bare MWCNT was easily peeled off from the substrate during ultrasonication or CV/EIS measurements, showing instability in experiments.

Using the electrode fabricated via the standard process, CV measurements of 4 mM $[Fe(CN)_6]^{3-}/[Fe(CN)_6]^{4-}$ in the PBS solution varying the scan rate from 0.05 to 0.6 V/s were conducted (see Fig. 2c). Figure 2d indicates that the magnitudes of both the anodic and cathodic peak currents (I_{pa} and I_{pc}, respectively) linearly increased with the square root of the scan rate (v); the fitting equations are $I_{pc}\ (\text{mA}) = -0.009 + 0.805 \times \upsilon^{1/2}$ with an $R^2 = 0.9881$, and $I_{pa}\ (\text{mA}) = -0.081 - 0.712 \times \upsilon^{1/2}$ with an $R^2 = 0.9967$. This indicates that the redox reaction is diffusion controlled for using the MWCNT/PDMS electrode as a working electrode, and is suitable for quantitative electrochemical analysis (Ghoreishi et al., 2013; Rahman and Jeon, 2007).

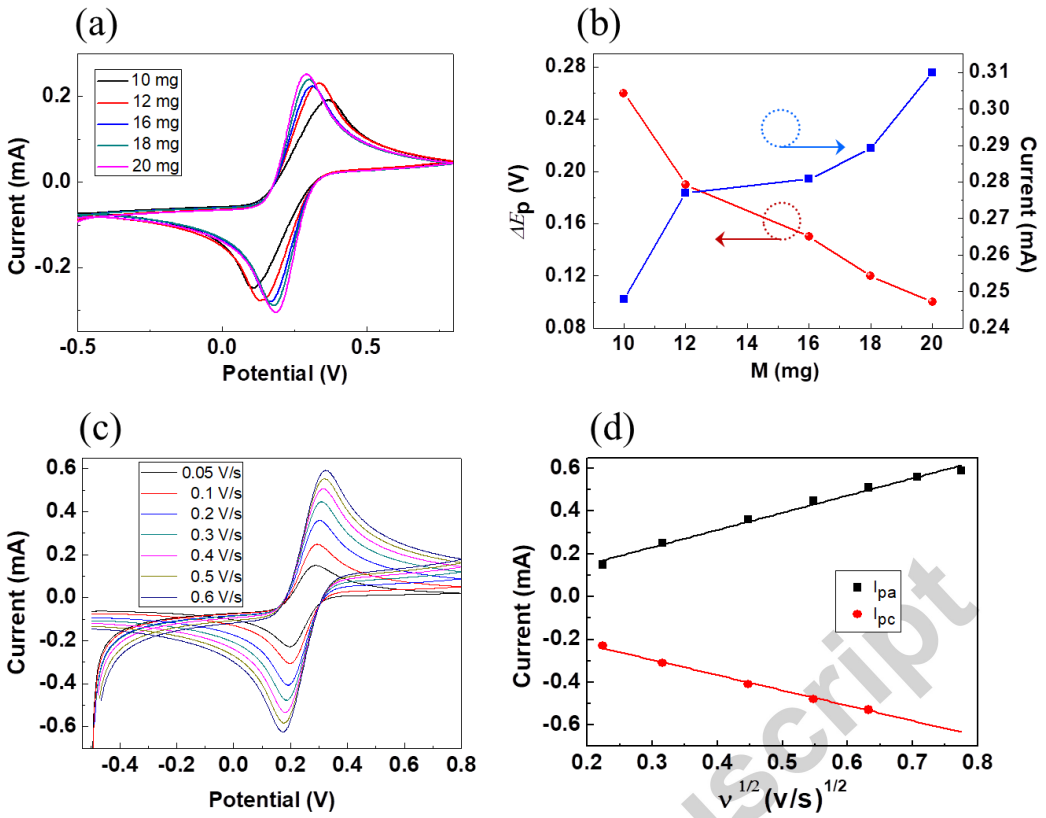

Fig. 2. (a) Cyclic voltammograms of 4 mM $[Fe(CN)_6]^{3-}$/$[Fe(CN)_6]^{4-}$ for the MWCNT/PDMS electrodes fabricated by varying the mass of the MWCNT and (b) the peak voltage separation (ΔE_p) and the anodic peak current in the voltammograms as a function of the mass of the MWCNT (M). (c) Cyclic voltammograms of 4 mM $[Fe(CN)_6]^{3-}$/$[Fe(CN)_6]^{4-}$ for a MWCNT/PDMS electrode with scan rates from 0.05 to 0.6 V/s and (d) cathodic and anodic peak currents (I_{pc} and I_{pa}, respectively) in the curves as a function of the square root of the scan rates (ν).

2.4 Measurements using EIS

In normal cases, DNA is only contained in cells in real blood and, thus, we assume that DNA is extracted from cells with other inteferents such as lipids and proteins filtered out before the DNA detection. We used PBS containing DNA as a

representative for purified samples. For DNA detection using EIS measurements, probe (P-DNA) and one of the targets (C-DNA, O-DNA, or A-DNA) were added to 1 mL of 1×PBS solution containing 4 mM $[Fe(CN)_6]^{3-}/[Fe(CN)_6]^{4-}$; the details of the probe and the target concentrations will be addressed later in this article for each experiment. The solution was maintained at room temperature for 5 min; we found that 5 min was sufficient for the hybridization reaction as indicated from the UV absorption measurements shown in Fig. S4. Then, 100 μL of the sample solution was placed onto the surface of the MWCNT/PDMS electrode, occupying approximately one-half of the electrode surface, as shown in Fig. 1c. Both the Ag/AgCl reference and platinum counter electrode were immersed into the sample solution while the bottom was retained at the same distance to the MWCNT surface and fixed as a constant for every measurement (see Fig 1c). The formal (or open circuit) potential of the electrode, i.e., the average of the potentials for anodic and cathodic peaks was *ca.* 0.24 V, as shown in the curve for using 16 mg MWCNT in Fig. 2a. Prior to EIS measurement, we applied a 0.24 V potential to the MWCNT/PDMS working electrode for 10 min to assist in DNA accumulation on the electrode, following the results shown in Fig. S5 in which the charge transfer resistance (R_{ct}) converged at 10 min after applying 0.24 V to the electrode. As a final step for DNA detection, EIS was performed in a frequency range from 1 Hz to 0.1 MHz, with an AC amplitude of 5 mV and a DC bias of the formal potential, i.e., 0.24 V. Because the EIS usually ended within 10 min, the total time required for detection of DNA was less than 30 min, including the DNA hybridization time (5 min) and the DNA accumulation time (10

min).

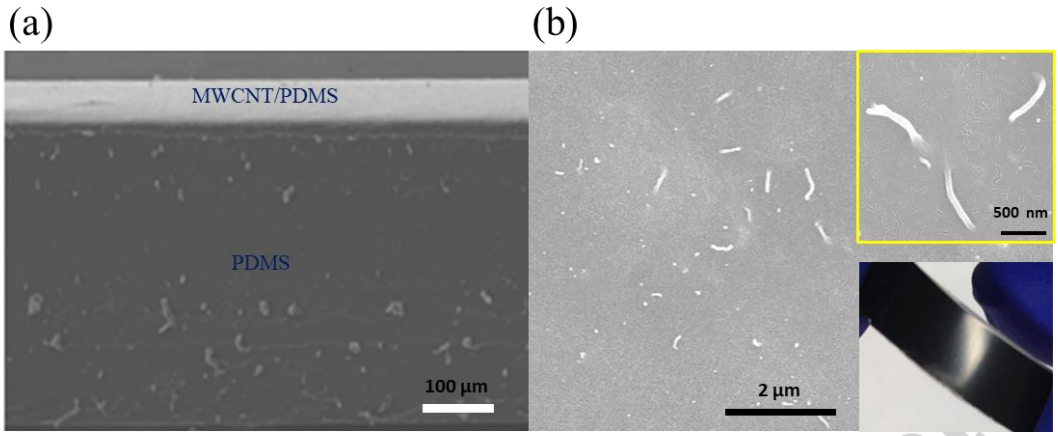

Fig. 3. (a) Cross section of the MWCNT/PDMS layer. (b) Micrograph of the surface of the MWCNT/PDMS electrode using SEM (the upper inset is a more magnified view and the lower one is the photograph of the electrode).

3. Results and discussion

1.1 Characterization of the MWCNT/PDMS electrode

The surface morphology and cross-section of the MWCNT/PDMS electrode was obtained using SEM (Fig. 3). The average thickness of the MWCNT/PDMS layer was estimated to be *ca.* 60 µm. The thickness of the layer was fairly uniform with no wrinkles, bubbles, and break points, as shown in Fig. 3a. The smooth surface of the MWCNT also can be seen in the lower inset (photograph) of Fig. 3b.

1.2 DNA detection mechanism

The mechanism of DNA detection using EIS is schematically illustrated in Fig. 1a. It has been reported that single-strand DNA (ss-DNA) is more likely to be absorbed

on the surface of a CNT via π-π stacking while double-strand DNA (ds-DNA) does not bind to a CNT (Star et al., 2006; Zhao and Johnson., 2007; Zheng et al., 2003). For A-DNA target, the sequences of the probe and the target are totally mismatched such that the single-stranded target and probe might be adsorbed onto the MWCNTs on the electrode via the π-π interaction (Star et al., 2006; Zheng et al., 2003). Because the adsorbed ss-DNA can act as a charge transfer barrier between the redox couple ($[Fe(CN)_6]^{3-}/[Fe(CN)_6]^{4-}$) and the MWCNTs, R_{ct} considerably increases. On the other hand, for the complementary target, C-DNA, ds-DNA can form via hybridization between C-DNA and P-DNA. Most of the ds-DNA remains far from the electrode rather than being adsorbed onto the MWCNT layer (Zhao and Johnson., 2007). Thus, the increase in R_{ct} is much smaller than that for the previous case in which A-DNA was used as a target. When O-DNA is used as a target, the probe and target have a single base mismatch. Because the degree of sequence mismatch is between those for C-DNA and A-DNA, R_{ct} would also lie between those for these two cases.

1.3 Selectivity of DNA biosensor

As shown in Fig. 4a, Nyquist plots for the 500 nM probe and 500 nM target were obtained using EIS. R_{ct} values, which were fitted via the equivalent circuit shown in the inset of Fig. 4a, were calculated as 6133, 9197, and 15976 Ω for targets C-DNA, O-DNA, and A-DNA, respectively, as shown in Fig. 4b; the largest R_{ct} was obtained for A-DNA, while the smallest was for C-DNA, in good agreement with the detection mechanism discussed in Section 3.2. Regarding the R_{ct} for the complementary target

(C-DNA), that for the one-base-mismatched target increased by 49.7%, indicating a high sequence selectivity in our system.

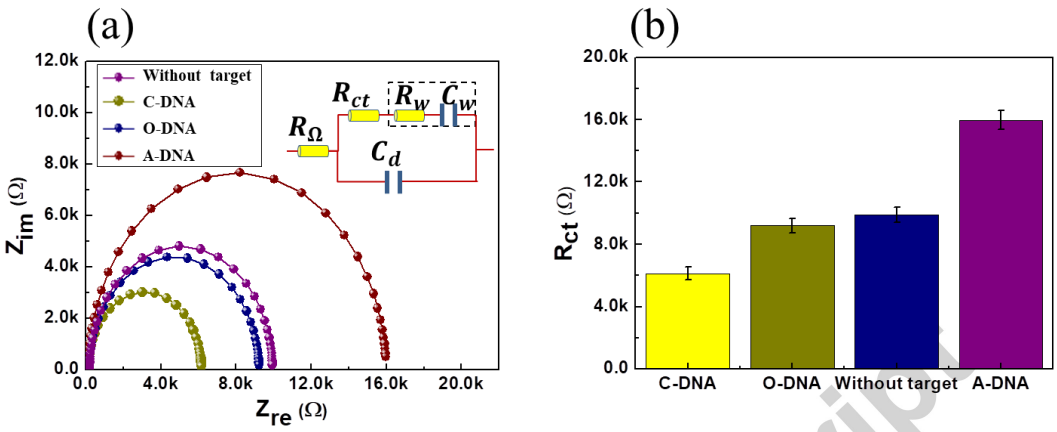

Fig. 4. (a) Nyquist plots and (b) R_{ct} values with probes such as C-DNA, O-DNA, and A-DNA and without any target.

1.4 Detection limit of the DNA sensor

We quantitatively analyzed the relationship between different concentrations of the target (C-DNA) and R_{ct} under high (1000 nM) and low (10 nM) probe (P-DNA) concentrations. For the 1000 nM probe, R_{ct} increased from 10246 to 14745 Ω with a decrease in the concentration of the target from 1000 to 10 nM (Fig. 5a). As shown in Fig. 5b, R_{ct} was proportional to the logarithm of the target concentration, indicating that our system is suitable for DNA quantification. The regression equation was fitted to be $R_{ct} = 1.74 \times 10^4 - 2.34 \times 10^3 \cdot \log C_1$ with an R^2=0.96603, where C_1 is the concentration of C-DNA ranging from 1000 to 10 nM. For the 10 nM probe, the relationship between R_{ct} and C_2 (C_2 is the concentration of the C-DNA ranging from 10 to 0.05 nM) was also investigated in the same manner as previously mentioned and

as shown in Fig. 5c. Similar to R_{ct} for the 1000 nM probe, that for the 10 nM probe was also proportional to the logarithm of the probe concentration, fitted to the equation $R_{ct} = 1.34 \times 10^3 - 1.20 \times 10^3 \cdot \log C_2$ with an R^2=0.9921, as shown in Fig. 5d. Because, here, we assumed that the concentrations of the target should be lower than that of the probe and thereby the maximum target concentration could be regarded as 10 nM. Thus, the linear range could be regarded as 0.05-10 nM for 10 nM probe, as shown in Fig. 5d. Detecting the DNA concentration higher than 10 nM was enabled by increasing the probe concentration; as shown in Fig. 5b, the linear range for the target using 1000 nM probe was approximately 10-1000 nM. The limit of detection (LOD) was estimated to be 25 pM (S/N=3). Note that 10 nM probe was used to determine the detection limit, while the assay using 1000 nM probe was the example that showed that the linear range could be shifted to high concentration region by increasing the probe concentration. Compared to the previous study, in which the MWCNT/PDMS was used as a working electrode for DNA detection in DPV (Li and Lee, 2015), the LOD decreased by more than five times, and the time required for DNA detection decreased from 1 h to less than 30 min. As listed in Table. S2, the detection time of our system is shorter and, moreover, the selectivity for one-base mismatch, which is defined as (R_{ct} for one base-pair mismatch)/(R_{ct} for no base-pair mismatch), is 1.3-6.5 times higher than those of other EIS-based sensors. The LOD of this study is less than that (50 pM) of some DNA sensors based on EIS and CNTs (Henihan et al., 2016), but higher than that (23 fM) of other sensors (Gong et al., 2017). Considering that most of the EIS-based DNA sensors using CNTs

require laborious and inefficient surface modification and probe immobilization processes (Henihan et al., 2016; Gong et al., 2017), the LOD of our sensor is highly competitive with those of other sensors based on EIS and CNTs. In addition, because the fabrication process is relatively simple compared to that of other CNT-based sensors, our sensor system is promising for mass production with uniform performance.

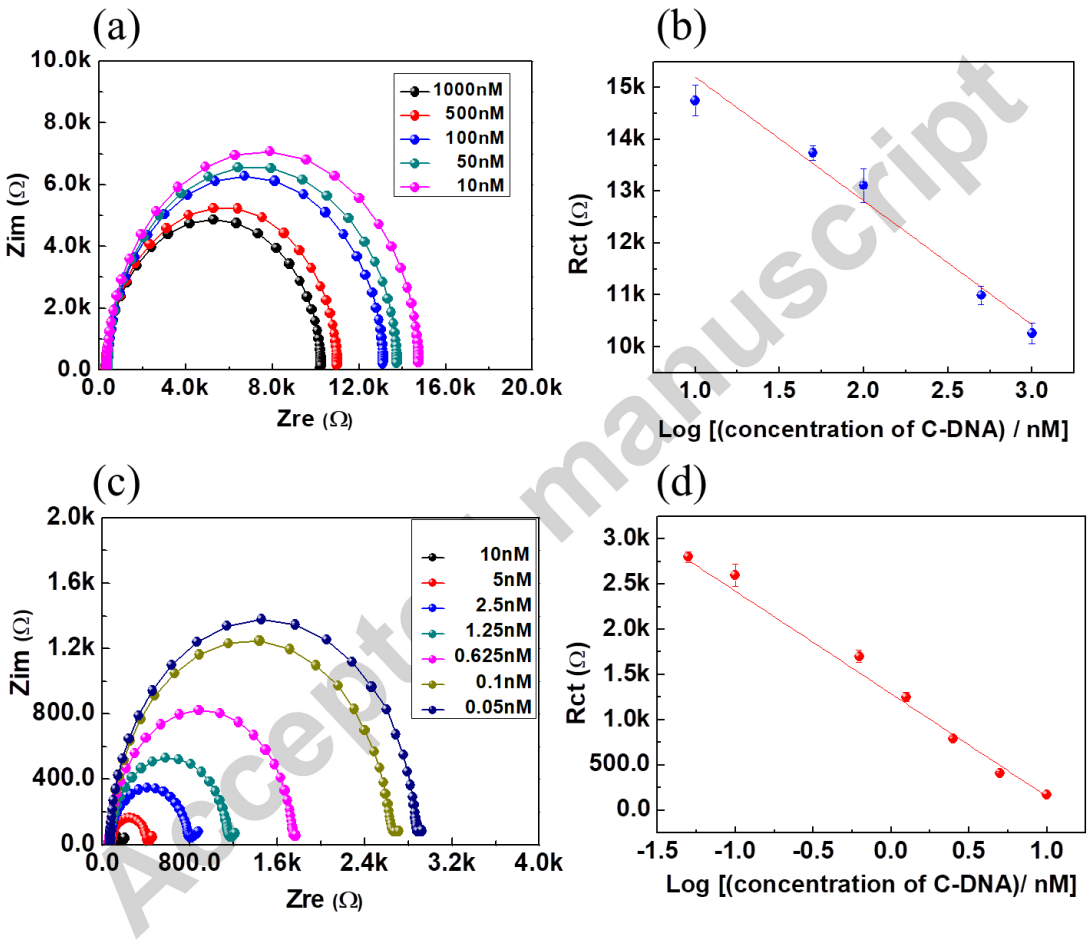

Fig. 5 (a) Nyquist plots for the 1000 nM probe and various target (C-DNA) concentrations and (b) R_{ct} extracted from these graphs as a function of target concentration. (c) Nyquist plots for the 10 nM probe and various target (C-DNA) concentrations and R_{ct} extracted from these curves as a function of target concentration.

1.5 Reusability and stability of the electrode

The reusability of our DNA sensor was investigated by repeating the same EIS measurements five times using the same MWCNT/PDMS electrode. During the experiment, 100 μL of sample solution containing 10 nM probe without any target was placed on the surface of the MWCNT electrode, followed by EIS measurement as mentioned in section 2.4. Between each experiment, the electrode was regenerated by ultrasonication in absolute ethanol for 2 min and in DI water for 3 min; here, ethanol was included because it is a widely used disinfectant in medical diagnosis. As shown in Fig. 6a, the Nyquist plots for the five experiments were stably obtained, and the relative standard deviation of the five R_{ct} values was 3.55% (Fig. 6b). As discussed above, ssDNA is physically absorbed on MWCNT through π- π stacking interactions. Because the strength of the physical adsorption is weaker than that of chemical adsorption, ssDNA possibly comes off from MWCNT by cleanings such as ultrasonication in ethanol and DI water. On the other hand, as shown in Fig. 3b, MWCNTs were strongly attached to the PDMS. Thus, MWCNTs cannot be removed from PDMS by ultrasonication in ethanol and DI water. These are confirmed by additional experiments, whose results are exhibited in Fig. S6; when EIS measurements for 100 μL of PBS solution containing 4 mM of the redox couple were conducted using both fresh and regenerated electrodes, the impedance of the regenerated electrode was only 3.12 % larger than that of the fresh one, indicating that the DNA on the regenerated electrode was cleanly removed by the ultrasonication, while MWCNTs on the surface were little affected. Because our MWCNT electrode is

stable when cleansed using water, ethanol, or ultrasonication, it may be robust against various cleaning processes removing DNA and chemicals from the electrode and, thereby, is promising as a reusable DNA sensor.

We also measured the R_{ct} values of five independently fabricated electrodes and found that the relative standard deviation was only 3.63% (Fig. S7a), indicating good reproducibility of the electrode. The stability for 7 days was investigated by measuring (average) R_{ct} every day as shown in Fig S7b. The relative standard deviation of R_{ct} is 1.68%, indicating good stability of the electrode.

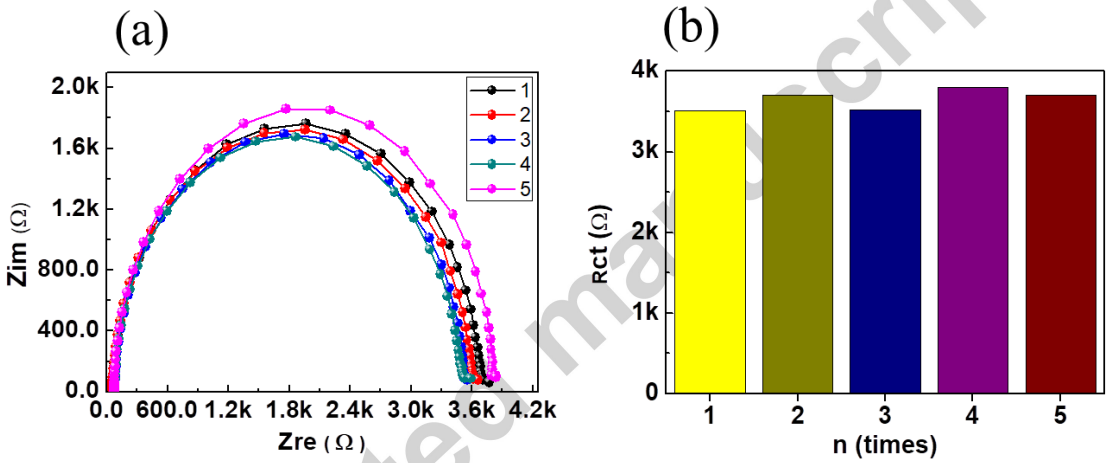

Fig. 6 (a) Nyquist plots for five independent experiments. (b) Histogram of R_{ct} of five experiments.

2. Conclusion

An electrochemical impedimetric DNA detection free from probe immobilization and surface modification was achieved using EIS for the flexible MWCNT/PDMS composite electrode. The electrode was found to be stable when cleansed by water, ethanol, and ultrasonication, showing its good reusability. Compared to previous

DPV-based DNA detection using a similar electrode, the measurement time decreased from 1 h to 30 min, and the LOD decreased from 130 to 25 pM. We cannot rule out the possibility that LOD is decreased by further optimization. Even single base-pair mismatches could be detected using this sensor system. These results show that the MWCNT/PDMS composite electrode can be successfully applied in EIS-based DNA detection. Because of simple fabrication process, our sensor system is suitable for mass production, suggesting a significant commercial potential. Detection of cell-free DNA from cancers or circulating tumor DNA in blood serum using this electrode is the topic of our future research.

Acknowledgements

This work was supported by the National Research Foundation of Korea (NRF) funded by the Ministry of Science and ICT (Grant No. 2016R1A2B2015389).

References

Bergin, S.D., Sun, Z., Streich, P., Hamilton, J., Coleman, J.N., 2010. J. Phys. Chem. C. 114, 231-237

Brett, CM. A., Brett, A. M. O., Serrano, SH. P., 1999. Electrochim. Acta. 44, 4233-4239

Chen, M., Hou, C., Huo, D., Bao, J., Fa, H., Shen, C., 2016. Biosens. Bioelectron. 85, 684-691

Cui, M., Wang, Y., Wang, H., Wu, Y., Luo, X., 2017. Sens Actuators B Chem. 244, 742-749

Drummond, T. G., Hill, M. G., Barton, J. K., 2003. Nat. Biotechnol. 21, 1192-1199

Fu, Y., Yuan, R., Xu, L., Chai, Y., Zhong, X., Tang, D., 2005. Biochem. Eng. J. 23, 37-44

Galan, T., Prieto-Simon, B., Alvira, M., Eritja, R., Gotz, G., Bauerle, P., Samitier, J., 2015. Biosens. Bioelectron. 74, 751-756

Garrido-Cardenas, J. A., Garcia-Maroto, F., Alvarez-Bermejo, J. A., Manzano-Agugliaro, F., 2017. Sensors. 17, 588

Ghoreishi, S. M., Behpour, M., Hajisadeghian, E., Golestaneh, M., 2013. J. Chil. Chem. Soc. 58, 1513-1516

Gong, Q., Wang, Y., Yang, H., 2017. Biosens. Bioelectron. 89, 565-569

Gupta, V. K., Yola, M. L., Qureshi, M. S., Solak, A. O., Atar, N., Ustundag, Z., 2013. Sens Actuators B Chem. 188, 1201-1211

Hassen, W. M., Chaix, C., Abdelghani, A., Bessueille, F., Leonard, D., Jaffrezic-Renault, N., 2008. Sens Actuators B Chem. 134, 755-760

Henihan, G., Schulze, H., Corrigan, D.K., Giraud, G., Terry, J.G., Hardie, A., Campbell, C.J., Walton, A.J., Crain, J., Pethig, R., Templeton, K.E., Mount, A.R., Bachmann,T.T., 2016. Biosens. Bioelectron. 81, 487–494

Heller, M.J., 2002. Annu. Rev. Biomed. Eng. 4: 129-153

Huang, K., Wang, L., Zhang, J., Wang, L., Mo, Y., 2014. Energy. 67, 234–240

Iijima, S., 1991. Nature. 354, 56–58

Keighley, S. D., Estrela, P., Li, P., Migliorato, P., 2008. Biosens. Bioelectron. 24, 906-911

Khan, W.A., Khan, Z.H., Rahi, M., 2014. Appl. Nanosci. 4, 633–641

Li, A., Yang, F., Ma, Y., Yang, X., 2007. Biosens. Bioelectron. 22, 1716-1722

Li, F., Pei, H., Wang, L., Lu, J., Gao, J., Jiang, B., Zhao, X., Fan, C., 2013. Adv. Funct. Mater. 23, 4140-4148

Li, J., Lee, E-C., 2015. Biosens. Bioelectron. 71, 414-419

Ma, K., Wang, H., Li, H., Xu, B., Tian, W., 2017. Sens Actuators B Chem. 253, 92-96

Mcglennen, R. C., 2001. Clin. Chem. 47, 393-402

Noimark, S., Colchester, R. J., Blackburn, B. J., Zhang, E. Z., Alles, E. J., Ourselin, S., Beard, P. C., Papakonstantinou, I., Parkin, I. P., Desjardins, A. E., 2016. Adv. Funct. Mater. 26, 8390-8396

Peng, H-P., Hu, Y., Liu, P., Deng, Y-N., Wang, P., Chen, W., Liu, A-L., Chen, Y-Z., Lin, X-H., 2015. Sens Actuators B Chem. 207, 269-276

Pumera, M., Merkoçi. A., Alegret, S., 2006. Sens Actuators B Chem. 113,617–622

Rahman, M. M., Jeon, I. C., 2007. J. Braz. Chem. Soc. 6, 1150-1157

Ramanathan, M., Patil, M., Epur, R., Yun, Y., Shanov, V., Schulz, M., Heineman, W.R., Datta, M.K., Kumta, P.N., 2016. Biosens. Bioelectron. 77, 580–588

Star, A., Tu, E., Niemann, J., Gabriel, J. C., Joiner, C. S., Valcke, C., 2006. Proc. Natl. Acad. Sci. USA. 103, 921-926

Weber, J. E., Pillai, S., Ram, M. K., Kumar, A., Singh, S. R., 2011. Mater. Sci. Eng. C. 31, 821-825

Xu, Y., Ye, X., Yang, L., He, P., Fang, Y., 2006. Electroanalysis. 15, 1471-1478

Yang, J., Yang, T., Feng, Y., Jiao, K., 2007. Anal. Biochem. 365, 24-30

Zhao, X., Johnson, J. K., 2007. J. Am. Chem. Soc. 129, 10438-10445

Zheng, M., Jagota, A., Semke, E. D., Diner, B. A., Mclean, R. S., Lustig, S. R., Richardson, R. E., Tassi, N. G., 2003. Nat. Mater. 2, 338-342

Highlights

- Carbon nanotube / polymer electrodes were simply fabricated using all-solution processing.
- The bare electrodes act as a recognition layer for DNA in electrochemical impedance spectroscopy.
- Single base-pair mismatches between the target and probe could be detected.
- The electrodes are reusable via a simple cleansing process.